MINIMUM TOTAL VARIATION IN 3D ULTRASOUND RECONSTRUCTION

João Sanches José M. Bioucas-Dias Jorge S. Marques

Instituto Superior Técnico
Instituto de Telecomunicacões
Instituto de Sistemas e Robótica
Lisbon, Portugal

ABSTRACT

The paper proposes a Bayesian 3D ultrasound reconstruction/estimation from non-uniform ultrasound observations, non-Gaussian data fidelity term, and *total variation* (TV) based prior. To compute the *maximum a posteriori* (MAP) solution, we introduce a Generalized Expectation Maximization (GEM) algorithm, which converges to the exact MAP solution in the case of convex data fidelity term. A set of experiments illustrates the effectiveness of the method.

1. INTRODUCTION

Three dimensional (3D) ultrasound aims at reconstructing 3D regions of the human body from a set of non-parallel cross sections degraded by multiplicative noise [1]. Most 3D ultrasound reconstruction methods adopt heuristic interpolation techniques aiming at real time operation in interactive medical diagnosis (see, e.g., [2]).

l^2 norm has been extensively used to regularize the reconstructed solution, as it leads to a linear set of equations, provided that the data is Gaussian. However, this norm tends to oversmooth the transitions between regions. This problem has been attacked using discontinuity-preserving priors (regularization terms) under the Bayesian (regularization) framework [5], [3],[4]

This paper proposes a new Bayesian approach to the reconstruction of 3D volumes from ultrasound data, where the prior on the function to be reconstructed, $F \equiv \{f_1, ..., f_N\}^T$, is defined as

$$p(F) = \frac{1}{Z} e^{-\alpha \sum_{\{p,q\}\in\mathcal{N}} |f_p - f_q|}, \qquad (1)$$

where $\mathcal{N}$ denotes the set of adjacent nodes in $P \equiv \{1, 2, ..., N\}$, Z is a normalizing constant, and $\alpha > 0$ controls the prior strength. The term $TV \equiv \sum_{\{p,q\}\in\mathcal{N}} |f_p - f_q|$ is the so-called *Total Variation* of F [6]. Abrupt variations on f_i are less penalized by TV than by l^2 norm. Therefore, discontinuities are better preserved by using the former prior.

Correspondent author: J. Sanches (jmrs@alfa.ist.utl.pt)

TV based reconstruction usually leads to a set of non-linear equations, even in the case of Gaussian observation models. Herein, we overcome this difficulty by designing an iterative Generalized Expectation Maximization (GEM) algorithm inspired by the methodology developed in [9].

The paper is organized as follows. Section 2 formulates the problem. Section 3 addresses the optimization procedures, and section 4 presents experimental results.

2. PROBLEM FORMULATION

Let $f : R^n \longrightarrow R$ be a function to be estimated from a set of M noisy observations, y_i, acquired at correspondent locations $x_i, 1 \leq i \leq M$. The specification of the sampling coordinates allows to deal with a wide range of problems, such as 3D ultrasound where an unknown 3D function is estimated from non-uniform sampled data.

2.1. Function representation

It is assumed that $f(x)$ belongs to a finite dimension linear space, being represented as a linear combination of basis functions $\phi_i(x)$, i.e.,

$$f(x) = \sum_{i=1}^{N} f_i \phi_i(x) = \Phi(x)^T F, \qquad (2)$$

where $\Phi(x) \equiv \{\phi_1(x), \phi_2(x), ..., \phi_N(x)\}^T$ is a N-dimensional vector containing the basis functions. The basis functions are shifted versions of a mother function, $\phi(x)$, centered at the nodes of a regular grid, i.e., $\phi_i(x) = \phi(x - \mu_i)$, where μ_i is the location of the i-th node.

2.2. Data model

The noisy observations are assumed to be independent. Two models for the noise are considered: 1) white additive Gaussian and 2) white multiplicative Rayleigh. The statistical independence may not be realistic in some cases. However, it is a convenient hypothesis because it simplifies a lot the

expressions and their inclusion in the mathematical formulation may not lead to relevant improvement on the final solution, as noted in [7]. Finally, it is assumed that the locations x_i are accurately known. Therefore, the acquisition process, in the case of the additive model (the multiplicative model is considered later in Section 3), can be formulated as

$$y_i = f(x_i) + \eta_i, \tag{3}$$

where $p(\eta_i) = \mathcal{N}(0, \sigma^2)$. In vector notation, we have

$$Y = \Psi F + \Gamma, \tag{4}$$

with $Y \equiv \{y_i\}$, $\Psi \equiv \{\Phi(x_1), \Phi(x_2), ..., \Phi(x_N)\}^T$ being an $M \times N$ matrix, and $\Gamma \equiv \{\eta_1, \eta_2, ..., \eta_M\}^T$ a column vector of dimension M.

The log-likelihood function is therefore

$$\begin{aligned} l(F) &\equiv \log\left[\prod_{i=1}^{M} p(y_i|x_i, f_i)\right] && (5)\\ &= C - \frac{1}{2\sigma^2}\sum_{i=1}^{M}\left[f(x_i) - y_i\right]^2 && (6)\\ &= C - \frac{1}{2\sigma^2}\|\Psi F - Y\|_2^2, && (7)\end{aligned}$$

where C is a constant.

2.3. Prior density

Let us define the matrix Θ such that $\Delta = \Theta F$, where Δ is a column vector containing all differences $f_p - f_q$, for $\{p, q\} \in \mathcal{N}$. The prior (1) is then given by

$$p(F) = \frac{1}{Z}e^{-\alpha\|\Delta\|_1} = \frac{1}{Z}e^{-\alpha\|\Theta F\|_1}.$$

2.4. MAP solution

The MAP estimation of F is

$$\widehat{F} = \arg\max_F [L(F)], \tag{8}$$

where

$$L(F) \equiv \log\left[p(Y|F)\right] + \log\left[p(F)\right] + C, \tag{9}$$

with C being a constant. Therefore,

$$L(F) = -\frac{1}{2\sigma^2}\|\Psi F - Y\|_2^2 - \alpha\|\Theta F\|_1. \tag{10}$$

The MAP estimate is then given by

$$\widehat{F} = \arg\max_F \left[L(F)\right] \tag{11}$$

3. OPTIMIZATION

The huge dimension of F (F is defined on a 3D grid) and the mixture of the l_1 and l_2 norms make the optimization of (11) very hard from the computational point of view. To overcome this difficulty, we propose an EM scheme. The EM algorithm [8] yields a non-decreasing log-posteriori sequence, $\{L(F_t), t = 0, 1, ...\}$, where $\{F_t, t = 0, 1, ...\}$ is generated by the two following step iteration:

1. E-step: - $Q(F, F_t) \equiv E[\log p(Y, Z, F)|Y, F_t]$
2. M-step: - $\widehat{F} = \arg\max_F \{Q(F, F_t)\}$.

The random vector Z is the so-called missing data. Herein, we follow the ideas presented in [9] where $Z = \{z_i\}$ plays the role of a scale factor in a Gaussian decomposition of the prior. More specifically, from (8) we see that the components of the random vector $\Delta \equiv \{\delta_i\}$ are independent and Laplacian distributed. This density admits the decomposition (see, e.g., [9])

$$p(\delta_i) = E_{z_i}[p(\delta_i|z_i)], \tag{12}$$

where $p(\delta_i|z_i) = \mathcal{N}(0, z_i)$ and $p(z_i) = \alpha e^{-\alpha z_i}$, for $z_i > 0$. With this setting, and following [9] we obtain:

$$Q(F, F_t) = -\frac{1}{2\sigma^2}\|\Psi F - Y\|^2 - \frac{1}{2}\Delta^T D_t \Delta, \tag{13}$$

where $D_t \equiv \{d(\delta_{ti})\}$ (see footnote[1]), $d(\delta) = -\frac{1}{\delta p(\delta)}\frac{dp(\delta)}{d\delta} = \alpha|\delta|^{-1}$, and

$$F_{t+1}^T = (\Psi^T\Psi + \sigma^2\alpha\Theta^T D_t\Theta)^{-1}\Psi^T Y. \tag{14}$$

The maximization of (13) amounts therefore to solve a quadratic problem.

3.1. Implementation

The solution of equation (14) is obtained by inverting an huge matrix, which is unpractical. To circumvent this difficulty, we use the Gauss Seidel algorithm, which optimizes (13) with respect to only an unknown at a time, keeping the remaining variables constant. This approach leads to the following recursion

$$\begin{aligned} f_{(t+1)i} &= \frac{1}{W_{ti}}\sum_{j\in S_i}\left[f_t(x_j) - y_j\right]\phi_i(x_j) + \bar{f}_{ti} && (15)\\ \bar{f}_{ti} &= \frac{1}{W_{ti}}\sum_{q\in\mathcal{V}_i} w_{tiq} f_{tq} && (16)\\ W_{ti} &= \sum_{q\in\mathcal{V}_i} w_{tiq} && (17)\end{aligned}$$

[1] The notation $(\cdot)_{ti}$ stands for the tth time instant for the ith component.

where $w_{tiq} \equiv \alpha|f_{ti} - f_{tq}|^{-1}$, $q \in \mathcal{V}_i$ is the set of adjacent nodes of node i and S_i is the set of sampling locations such that $\phi_i(x_j) \neq 0$. The parameter σ^2 was incorporated in the parameter α.

Notice that each component-wise optimization does not decrease the objective function (13). Therefore, after a full updating of F, we have $Q(F_{t+1}, F_t) \geq Q(F_t, F_t)$. The obtained scheme is thus a *Generalized Expectation Maximization* (GEM) algorithm, assuring therefore that the sequence $\{L(F_t), t = 0, 1, ...\}$ is still non-decreasing.

Observation densities other than Gaussian can be dealt with by using a similar approach. For the case of ultrasound data, the observation density is well described by a Rayleigh distribution [10], i.e., $p(y) = \frac{y}{f} e^{-\frac{y^2}{2f}}$. Equation (13) is therefore

$$Q(F, F_t) = -\sum_{i=1}^{M} \left[\log(\Psi F)_i + \frac{y_i^2}{2(\Psi F)_i} \right] - \frac{1}{2} \Delta^T D_t \Delta. \tag{18}$$

where $(\Psi F)_i$ is the ith element of the vector ΨF. Its maximization with respect to component i leads to

$$f_{(t+1)i} = \frac{1}{2\alpha W_{ti}} \sum_{j \in S_i} \left[\frac{y_j^2 - 2f_t(x_j)}{f_t^2(x_j)} \phi_i(x_j) \right] + \bar{f}_{ti} \tag{19}$$

4. EXPERIMENTAL RESULTS

In this section we present three examples of application using synthetic and real data. In the synthetic case we use 1D data corrupted with white additive Gaussian noise. In the real case, ultrasound data is used. In this latter example, the noise is assumed to be Rayleigh distributed.

4.1. Denoising - Synthetic 1D data

In this first experiment we have generated a vector F with dimension $N = 250$ corresponding to a rectangular shaped function having the values $F_{high} = 128$ and $F_{low} = -128$. The observations are simulated by adding F with additive white noise $\mathcal{N}(0, 30^2)$. To compare the results of using TV and l_2 priors, we have computed the signal to noise ratio (SNR) of the estimats obtained with different values of α, for both priors. The results are displayed in Fig.1. The SNR is maximum at $\alpha = 0.75$ and $\alpha = 0.001$ for TV and l_2 priors, respectively. The reconstructions using both priors and the respective values of α are displayed in Fig.2. The best SNR of the reconstruction using the l_1 prior is higher ($24.4dB$) than the best obtained using the l_2 prior ($16.9dB$).

4.2. Denoising - 2D ultrasound image of the Heart

In this section we present an example of using an ultrasound image of the heart, i.e., a 2D problem. Fig.3.a) displays

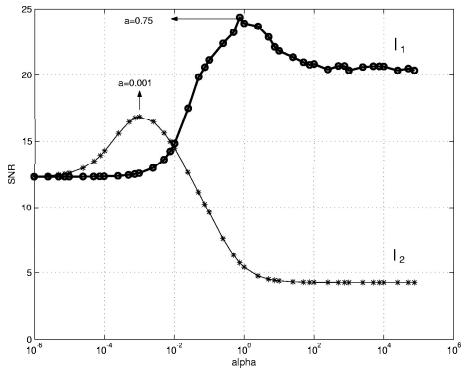

Fig. 1. $SNR(\alpha)$ of the reconstructions with synthetic data, obtained using the TV (thick line) and l_2 (thin line) based priors. 256 observations of a rectangular shaped function ($-128 < f(x) < 128$) corrupted by additive Gaussian noise, $\mathcal{N}(0, 30^2)$.

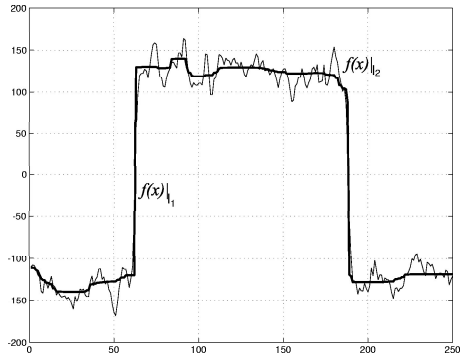

Fig. 2. Denoising results using TV (thick line) and l_2 (thin line) priors. 256 observations of the rectangular shaped function ($-128 < f(x) < 128$) corrupted by additive Gaussian noise, $N(0, 30^2)$.

an ultrasound image representing a cross section of a heart, where three chambers are visible. Fig's. a displays the original ultrasound image and Fig. b-d) and Fig. e-g) display the denoising results using the l_2 and TV based priors, respectively for $\alpha = 1, 10, 100$. As expected the results of using the TV prior leads to sharper solutions where the transitions appear better defined. Notice that TV reconstructions exhibit smaller sensitivity to the α then l_2 ones. This behavior can also be observed in Fig. 1 of 1D example.

4.3. Reconstruction - 3D Ultrasound (Gall Bladder)

In this last example we present the reconstruction results using the TV and l_2 priors. The observations are formed by 50 non-parallel ultrasound cross sections of a gall-bladder. These images were acquired by a conventional medical ultrasound equipment, to which an electromagnetic spatial locator was attached. This spatial locator gives the position

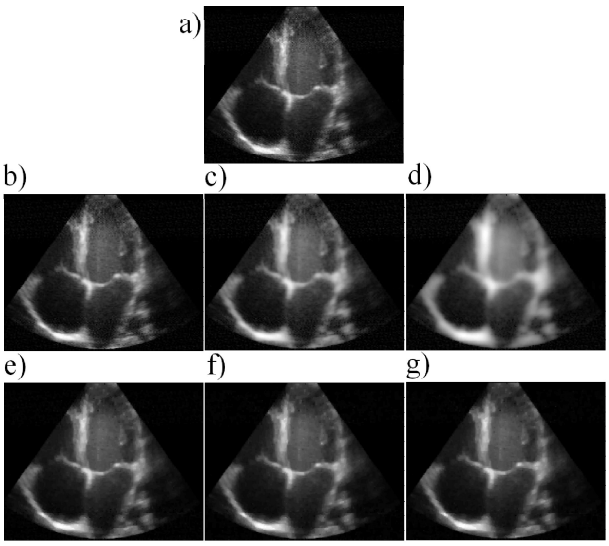

Fig. 3. Denoising of a heart ultrasound image. a)Ultrasound image. b-d)l_2 prior. e-g)TV prior for $alpha = 1, 10, 100$.

and orientation of the ultrasound probe, allowing the computation of the 3D position of each pixel on the ultrasound image. These positions and intensities are used with the Rayleigh distribution to compute the MAP estimates of the gall bladder anatomy.

The results are displayed in Fig.4. Column I shows three ultrasound images taken from the sequence and columns II and III show the correspondent cross sections extracted from the estimated volumes using l_2 and TV priors, respectively. Row d) shows new cross sections (with no correspondence on the original sequence) extracted from the reconstructed volumes embracing the whole organ. In the last row two surfaces, representing the organ border, are displayed. These two surfaces were obtained from the reconstructed volumes using both priors. As expected, TV prior leads to a better defined reconstructed organ, with sharper transitions.

5. CONCLUSIONS

This paper introduced a new Bayesian criterion to 3D ultrasound reconstruction. The prior, based on the Total Variation of the reconstructed function, is of edge-preserving type, a crucial goal in medical imaging. The MAP estimate is a complex optimization task, owing to the presence of Rayleigh density and TV prior. To overcame this difficulty, a GEM algorithm was designed, where each iteration solves a simple 1D optimization. The effectiveness of the method was illustrated by using synthetic and real data.

6. REFERENCES

[1] T.Nelson, D.Downey, D.Pretorius, A.Fenster,Three-Dimensional Ultrasound, Lippincott, 1999.

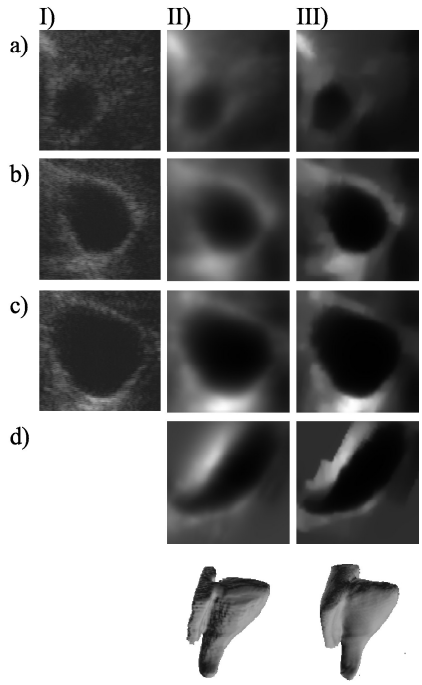

Fig. 4. Reconstruction - 3D Ultrasound. Reconstruction results from I)50 cross-sections of a gall-bladder using the l_2 (II) and the l_1 (III) priors.

[2] Rohling R., Gee A., Berman L.,Treece G., Radial basis function interpolation for 3D freehand ultrasound. Proc. of the 16th ICIPMI, pp.478-483, Visegrad, Hungary, June 1999.

[3] S. Alliney. An algorithm for the minimization of mixed l and l norms with application to bayesian estimation. IEEE Signal Processing, 42(3):618-627, 1994.

[4] S. Osher, A. Sole, and L. Vese. Image decomposition and restoration using total variation minimization and the H H norm. J. Mult. Model. and Simul., 1(3), 2003.

[5] M.J.Black, A.Rangarajan, On the unification of line processes, outlier rejection and robust statistics with applications in early vision, International Journal of Computer Vision, in press, 1996.

[6] C.R.Vogel, M.E.Oman, Fast, Robust Total Variation-Based Reconstruction of Noisy, Blurred Imges, IEEE Trans. on Image Processing, Vol.7, no.6, June 1998.

[7] E. Rignot, R. Chelappa, Segmentation of polarimetric sunthetic aperture radar data, IEEE Trans. Image Processing, vol.1, no.1, pp. 281-300, 1992.

[8] A.Dempster, N.Laird,D. Rubin, Maximum likelihood from incomplete data via the EM algorithm, Journal of the Royal Statistical Society, Series B, 39(1):1-38, 1977.

[9] J.Bioucas-Dias, Bayesian wavelet-based image deconvolution: a GEM algorithm, IEEE Transactions on Image Processing, In Press, 2005.

[10] C.Burckhardt, Speckle in Ultrasound B-Mode Scans, IEEE Trans. on Sonics and Ultrsonics, vol. SU-25, no.1, pp. 1-6, January 1978.